Protein Kinase A-Catalyzed Phosphorylation and Its Effect on Conformation in Phytochrome A†

Veniamin N. Lapko, Todd A. Wells, and Pill-Soon Song*

Department of Chemistry, University of Nebraska, Lincoln, Nebraska 68588-0304

Received December 13, 1995; Revised Manuscript Received March 26, 1996⊗

ABSTRACT: Phytochromes are ubiquitous red/far-red wavelength-sensitive photoreceptors in plants. Oat phytochrome A is a phosphoprotein. Phytochrome A (phyA) possesses two spatially different sites for phosphorylation with cAMP-dependent protein kinase (PKA) [McMichael & Lagarias (1990) *Biochemistry 29*, 3872−3878]. To assess the modulation of protein conformation by phosphorylation/dephosphorylation and its possible implication in phytochrome-mediated signal transduction, the conformations of phytochrome have been probed by PKA catalyzed phosphorylation. The phosphorylated species were purified and analyzed, along with untreated phytochrome, by limited proteolysis, circular dichroism (CD) and fluorescence quenching measurements. No significant changes in secondary structure of the phyA molecule after its phosphorylation were observed by CD. However, a subtle topographic and/or electrostatic effect of the phytochrome phosphorylation was detected by the time-resolved fluorescence quenching of Trp residues with Cs^+ ions. N-Terminal phosphorylation at Ser_{17} was unique to the Pr form, but both Pr and Pfr phytochromes were phosphorylated at the hinge region to some extent. Phosphorylation at the hinge region resulted in noticeable changes in the proteolytic patterns, inhibiting cleavage near the phosphorylation site and favoring tryptic digestion of the Lys_{536}-Asn_{537} peptide bond. Phosphorylation at the N-terminus did not cause observable changes in the helical structure of this region, but had an inhibitory effect on proteinase V8 accessibility at a site near the chromophore attachment. The functional relevance of protein phosphorylation of phyA is also discussed.

Phytochromes (phyA, B, C, D, and E; Hershey et al., 1985) are homodimeric photochromic proteins that serve as a light switch in regulating a great number of biochemical processes at various stages of plant development (Pratt, 1982; Quail, 1991; Furuya, 1993; Quail et al., 1995). The early molecular steps which follow the phototransformation of the red light absorbing form (Pr)[1] to the far-red light absorbing form (Pfr) are still undetermined. The possible involvement of phosphorylation in the light signal transduction mediated by phytochrome has been implicated (Park & Song, 1990; Romero et al., 1991a,b; Sommer and Song, personal communication). Protein kinase activity has been found to be part of/or associated with purified phytochrome (Wong et al., 1986; Grimm et al., 1989; Kim et al., 1989; Biermann et al., 1994). Phytochrome, itself, is a phosphoprotein (Quail et al., 1978; Hunt & Pratt, 1980). Phytochrome A is also phosphorylated by mammalian protein kinases, such as cAMP-dependent protein kinase, cGMP-dependent protein kinase, and Ca^{2+}-activated phospholipid-dependent protein kinase (Wong et al., 1986; McMichael & Lagarias, 1990).

Phytochromes are cytosolic proteins. It is possible that an initial event in the phytochrome-mediated signaling involves a post-translational modification of the photoreceptor itself. Protein phosphorylation can promote conformational changes in the proximity of/or at sites distant from the phosphoamino acid. These changes serve regulatory roles for enzyme activity and/or protein recognition. Gene transcription and translation, hormonal response, membrane transport, cell growth and division, and light harvesting are all intracellular processes controlled by phosphorylation (for review, see Johnson & Barford, 1993). No direct connection between phytochrome phosphorylation and signal transduction has been shown, but this receptor level post-translational modification may have far-reaching effects on signal transduction.

Studies on rhodopsin kinase (Wilden & Kuhn, 1982), β-adrenergic receptor kinase (Benovic et al., 1989), and β-adrenergic receptor kinase 2 (Benovic et al., 1991) suggest that receptor phosphorylation is a general mechanistic motif in G-protein coupled signal transduction. Mitchell et al. (1992) demonstrated that phosphorylation of rhodopsin did not affect the formation or stability of meta II, the active signal transducing form of rhodopsin. They suggest that conformational changes induced by phosphorylation disrupt the activation of transducin, increasing the rhodopsin−G_t dissociation constant by 10-fold. Like rhodopsin, phytochrome signal transduction may involve a G-protein receptor−phytochrome interaction (Romero et al., 1991a,b; Hahn & Song, 1991; Sommer & Song, 1993; Neuhaus et al., 1993). In the present study, we describe a detailed comparative analysis of phosphorylated (as Pr and Pfr) phytochrome and the untreated chromoprotein. The objective is to determine

† This work was supported by National Institutes of Health Grant GM-36956. Dedicated to Professor Horst Senger on his 65th birthday.

* To whom correspondence should be addressed.

⊗ Abstract published in *Advance ACS Abstracts,* May 15, 1996.

[1] Abbreviaitons: Pr and Pfr, red and far-red absorbing forms of phytochrome, respectively; SAR, specific absorbance ratio, A_{666}/A_{280}, with phytochrome in its red-absorbing form; PKA, cAMP-dependent protein kinase (catalytic subunit); PAGE, polyacrylamide gel electrophoresis; PBS, phosphate-buffered saline; PBS-T, phosphate-buffered saline containing 0.1% Tween-20; CD, circular dichroism; SDS, sodium dodecyl sulfate; ECL, enhanced chemiluminescence; PMSF, phenylmethanesulfonyl fluoride; EDTA, ethylenediaminetetraacetic acid; BSA, bovine serum albumin; TCA, trichloroacetic acid; Mab, monoclonal antibodies.

S0006-2960(95)02936-9 CCC: $12.00

if phosphorylation of Ser-17 and Ser-598 in phytochrome A causes detectable protein reorganization, thus further implicating phosphorylation as a regulatory mechanism in the light signaling pathway. Some phosphorylation events result in only steric blocking of binding sites or have no known function and are called "silent" phosphorylations. However, lack of phosphorylation induced conformational changes would not rule out a regulatory role, where the negatively charged phosphate group inhibits ligand or protein interaction by simply blocking the contact site sterically and/or electrostatically (Johnson & Barford, 1993).

MATERIALS AND METHODS

Reagents and Antibodies. Acrylamide, bis(acrylamide), SDS, and other chemicals for gel electrophoresis were obtained from Bio-Rad Laboratories (Richmond, CA). High range marker protein standards were obtained from Bio-Rad and low molecular weight standards from Pharmacia (Alameda, CA). Trypsin and proteinase from *Staphylococcus aureus* V8 were from Sigma Chemical Co. (St. Louis, MO), and ToyoPearl HW-65S was purchased from ToyoHaas (Montgomeryville, PA). Site-specific phytochrome monoclonal antibodies (Oat-22, Oat-25, and Pea-25) were the generous gift of Prof. L. H. Pratt. Horseradish peroxidase anti-mouse IgG conjugate was obtained from Promega (Madison, WI). Monoclonal anti-phosphotyrosine antibodies (clone IG2, 200 μg/mL), enhanced chemiluminescence (ECL) reagents kit, and Hyperfilm-ECL were from Amersham (Arlington Hills, IL). Phosphocellulose units for radioactive kinase assays were obtained from Pierce (Rockford, IL). [^{32}P]ATP (3000 Ci/mmol) as the tetrakis(triethylammonium) salt in 10 mM Tricine was purchased from NEN Research Products (Boston, MA). Con A Sepharose was obtained from Pharmacia Biotech. Calcium tartrate gel was prepared as described by Ahkrem and Drozhdenyuk (1989). All other chemicals were obtained from Sigma Chemical Co.

Phytochrome Preparations. Native 124-kDa phytochrome was purified from 3.5-day-old etiolated oat seedlings (*Avena sativa* L.) in the Pfr form as described recently (Lapko & Song, 1995), using two ammonium sulfate precipitation steps followed by ammonium sulfate back-extraction (ASBE) and gel filtration on Toyopearl HW-65. Specific absorbance ratio (A_{666}/A_{280}) of phytochrome preparations was 1.00−1.04.

A modification to our method was used to determine if phosphate content varies in different phytochrome preparations. Phytochrome with a SAR = 1.03 was prepared using the following procedure. All initial steps including ammonium sulfate precipitations were performed under green safety light with phytochrome as Pr, and then ASBE was performed with Pfr as indicated earlier.

A phytochrome preparation isolated as Pr (SAR = 0.74) was used to compare the autoradiographic data of tryptic digest for phytochrome purified as Pr with those for phytochrome purified as Pfr. Isolation of phytochrome in Pr form was performed essentially as described previously (Lapko, 1989) using two step chromatography on calcium tartrate gel, and DEAE-Toyopearl followed by gel filtration chromatography on Toyo-Pearl HW-65. All steps were performed under green safety light.

Protein Kinase A Preparation. The catalytic subunit of cAMP-dependent protein kinase (kinase A) was isolated from bovine heart according to Fletcher et al. (1986) with one exception, that calcium tartrate gel was used instead of hydroxyapatite. Kinase A had a specific activity of 600 nmol of phosphate incorporated into histone Type IIA min^{-1} (mg of protein)$^{-1}$ at 30 °C under standard conditions (Roskoski, 1983) as determined with Pierce phosphocellulose units. The stock solution, 0.8 mg/mL in 50 mM Tris-HCl buffer, pH 7.2, containing 0.1 mM EDTA and 5 mM 2-mercaptoethanol, was diluted to the desired concentration with 20 mM Tris-HCl buffer, containing 0.1 mM EDTA and 1 mg/mL bovine serum albumin, and 10 μL of the solution was used for radioactive phosphorylation measurements. For limited proteolysis experiments, the kinase A stock solution was diluted 10 times with 20 mM Tris-HCl buffer, pH 7.4, before use.

Prostatic acid phosphatase was purified from human prostatic adenoma tissue using concanavalin A chromatography and affinity chromatography on L-tartrate sepharose essentially as described by Van Etten et al. (1978). Activity of prostatic acid phosphatase was 550 μU/mg measured with *p*-nitrophenyl phosphate as the substrate at pH 5.0 or 250 μU/mg in 20 mM Tris-HCl buffer, pH 7.5 (25 °C).

Preparation of Dephosphorylated Phytochrome. Phytochrome solution [1.5 mL (1.5mg); 0.4 mol of phosphate/mol] was incubated as Pr at room temperature with 20 μg of prostatic acid phosphatase for 45 min and then for an additional 45 min as Pfr. Dephosphorylated phytochrome was isolated by passing the reaction mixture through a 0.7 × 2.0 cm Con A column equilibrated with 20 mM Tris-HCl buffer, pH 7.6, containing 1 mM $CaCl_2$, 1 mM $MgCl_2$, and 0.2 mM $MnCl_2$. The unbound phytochrome fraction was desalted on Bio-Gel P-6 in 20 mM Tris-HCl buffer, pH 7.5. The same conditions were used for phytochrome dephosphorylation with alkaline phosphatase and isolation of the dephosphorylated protein. Prior to use, alkaline phosphatase (Sigma Chemical Co.) was passed through a concanavalin A column and the fraction eluted with 100 mM methyl D-glycopyranoside (approx. yield 20%) was used for dephosphorylation.

Radioactive Phytochrome Phosphorylation Assay. The phosphorylation mixture was comprised of 1 mg/mL phytochrome (Pr or Pfr) in 20 mM Tris-HCl buffer, pH 7.5, containing 0.2 mM EDTA, 2 mM $MgCl_2$, 1 mM 2-mercaptoethanol, and 150 μM [^{32}P]ATP (400 cpm/pmol). The reaction was initiated by adding 10 μL of kinase solution (diluted with 0.1% BSA to ensure the desired enzyme:phytochrome ratio) and performed at 30 °C. At different time points, 10 μL of reaction mixture was added to 20 μL of 25 mM EDTA in 20 mM Tris buffer, pH 7.5, and 25 μL of the quenched mixture was used for determination of [^{32}P] incorporation using Pierce phosphocellulose separation units for radioactive kinase assay according to the manufacturer's recommendation.

Isolation of Phosphorylated Phytochrome Species. Thirty-six microliters of kinase A (0.8 mg/mL) was added to 3 mL of native phytochrome in the Pr or the Pfr form (0.9 mg/mL, phosphate content 0.4 mol/mol) in 20 mM Tris-HCl buffer, containing 2 mM $MgCl_2$, 0.2 mM EDTA, 1 mM 2-mercaptoethanol, and 150 μM ATP. After 1 h at 30 °C, the reaction mixture was quenched by addition of 330 μL of 150 mM EDTA in 20 mM Tris-HCl buffer (pH 7.5) and passed through a Bio-Gel P-6 column (2.5 × 8 cm) equilibrated with 20 mM Tris-HCl buffer, pH 7.5, containing 0.2 mM EDTA (buffer A) to remove most of the ATP which

interferes with reliable further separation. The phytochrome fraction was applied to a calcium tartrate gel column (0.7 × 3.5 cm) equilibrated with buffer A. The column was washed with 10 mL of buffer A, and the phytochrome was eluted with 60 mM phosphate buffer, pH 7.8, containing 0.2 mM EDTA. The phytochrome fraction was passed through a Bio-Gel P-6 column (1.5 × 12 cm) equilibrated with buffer A. The collected phytochrome fractions were concentrated if necessary using Centriprep-30 concentrator (Amicon) and stored at −70 °C in small aliquots.

Phytochrome Phosphorylation with [^{32}P]ATP for Autoradiography. To 190 μL of phytochrome as Pr or Pfr solution (1.5 mg/mL) in 20 mM Tris-HCl buffer, containing 0.3 mM EDTA (pH 7.5), were added 32 μL of 20 mM $MgCl_2$ (in 100 mM Tris-HCl buffer, containing 10 mM 2-mercaptoethanol, pH 7.5) and 47 μL of kinase A solution (diluted 10 times). The reaction was initiated by addition of 48 μL of 1000 μM [^{32}P]ATP (300 cpm/pmol) in 20 mM Tris-HCl buffer, pH 7.5. After incubation for 1 h at 30 °C, the reaction was terminated by addition of 35 μL of 150 mM EDTA in 20 mM Tris-HCl buffer, pH 7.5, and half of each reaction mixture was used for digestion in the form treated with PKA. The other half of each sample was converted to the other photoisomer by saturating red or far-red light before digestion. Since proteolytic patterns (with trypsin and proteinase V8) for purified phosphorylated phytochrome (ATP, kinase A, and EDTA were removed) were indistinguishable from those obtained for corresponding preparations directly digested in quenched reaction mixture, [^{32}P]-labeled phytochrome forms were used for digestion without repurification from the reaction mixture.

Limited Proteolysis. Phytochrome preparations (Pr phosphorylated, Pfr phosphorylated, and untreated phytochrome, each in the Pr or Pfr form), 0.8 mg/mL, in 20 mM Tris-HCl buffer containing 0.5 mM EDTA (pH 7.5) were used for tryptic digestion at 0 °C. The trypsin:phytochrome ratio was 1:2000 (w/w). Trypsin (2.5 mg) was dissolved in 2.5 mL of cold H_2O (pH 4.5, adjusted with HCl), placed in microcentrifuge tubes (50 μg/tube), lyophilized, and stored at −70 °C. Just before use, the trypsin was dissolved in 20 mM Tris-HCl buffer (pH 7.5) to the desired concentration, and 10 μL of the resulting solution was added to each phytochrome preparation. For every set of tryptic digests, a new portion of lyophilized enzyme was used. At different time points 20 μL of the reaction mixture was taken out and quenched with PMSF (final concentration 2 mM). After 10 min, the quenched solution was diluted with 25 μL of SDS−PAGE sample buffer, boiled for 2 min, and stored at −70 °C. Phytochrome digestion with proteinase V8 at an enzyme: phytochrome ratio 1:40 (w/w) was performed at the same conditions described for tryptic digest.

Preparation of Phosphotyrosine−Bovine Serum Albumin Conjugate. Thirty milligrams of 1-ethyl-3-(3-(dimethylamino)propyl)carbodiimide (EDAC) was added (3 × 10 mg in 15 min) to 10 mL of water containing 2.5 mg of bovine serum albumin and 0.5 mg of phosphotyrosine (pH 6.0). After 45 min at room temperature, 500 mg of glycine was added to the reaction mixture, and it was concentrated to 1.5 mL using a Centriprep-30 concentrator (Amicon) and desalted on a Bio-Gel P-6 column (1.5 × 10 cm) in 20 mM Tris-HCl buffer (pH 7.6). The phosphotyrosine content of the conjugate, 0.42 mol/mol of BSA, was determined by phosphate analysis after ashing.

Phosphate Determination. Phytochrome solution (300−400 μL; 2.5−3.0 nmol) was precipitated with an equal volume of 20% TCA at 0 °C. After centrifugation (5 min, 5000*g*), 40 μL of 10% magnesium nitrate in ethanol was added to the precipitate. Ashing of the sample and the subsequent phosphate determination were performed as described by Buss and Stull (1983). For determination of acid labile phosphate, phytochrome precipitated with TCA was incubated with 300 μL of 10% TCA for 25 min (90 °C), chilled, centrifuged, and treated as indicated earlier. For phosphate analysis of dephosphorylated phytochrome, 0.5−0.7 mg of the chromoprotein was used.

Protein Assays. Phytochrome concentrations were calculated using a molar extinction coefficient at 668 nm of 1.32 × 10^5 M^{-1} cm^{-1} (Lagarias et al., 1987). All other protein concentrations were determined according to Bradford (1976) with bovine serum albumin as a standard.

SDS−PAGE. SDS−PAGE was performed according to the method of Laemmli (1970) employing 8% or 10% acrylamide. The protein bands were visualized with Coomassie Brilliant Blue R-250 or silver stained using the method of Blum et al. (1987).

Immunoblotting. Protein bands after SDS−PAGE were transferred to nitrocellulose membrane at 250 V for 1 h. The membrane was incubated for 1 h at room temperature in 5% skim milk in PBS, containing 0.1% Tween-20 (PBS-T), and then washed 4 × 10 min with PBS-T. The membrane was probed with a monoclonal phytochrome antibody (incubation for 45 min) and washed 4 × 10 min with PBS-T, and peptide bands, after incubation with anti-mouse horseradish peroxidase labeled secondary antibodies (45 min, 1:10 000 dilution) followed by 3 × 7 min washing steps with PBS-T, were visualized by ECL. The membrane was then stripped by incubation in 50 mM Tris-HCl buffer, pH 6.7, containing 100 mM 2-mercaptoethanol and 2% SDS, for 30 min at 50 °C and reprobed with other primary antibodies.

The following primary monoclonal antibodies (Pratt et al., 1988) were generously supplied by Dr. Lee Pratt and used for assignment of fragments: Pea-25 monoclonal antibodies, specific for the C-terminal part of phytochrome at a 1:2000 dilution; Oat-25 monoclonal antibodies specific to the N-terminus of oat phytochrome (dilution 1:7500); and Oat-22 monoclonal antibodies specific to the chromophore region of oat phytochrome at a 1:7500 dilution.

Phosphotyrosine Determination. Phytochrome preparations along with phosphotyrosine containing standards (phosphotyrosine-BSA conjugate diluted with non-modified protein) after gel electrophoresis were transferred to nitrocellulose membrane. The membrane was probed with phosphotyrosine monoclonal antibody (dilution 1:250), and band detection was performed according to the ECL protocol as described earlier.

Autoradiography. The Coomassie stained gels were wrapped with Saran Wrap and used to expose Kodak X-Omat AR film for 24 h at room temperature. For radiolabel quantitation of limited proteolysis fragments, protein bands after SDS−PAGE and transfer to nitrocellulose membrane were excised from the dried membrane, placed into vials with 7.5 mL of scintillation cocktail, and measured on a Packard 1900 TRI-CARB liquid scintillation analyzer.

Amino Acid Sequence Analysis. The 4 h Pr tryptic digest was subjected to 8% SDS−PAGE and transferred to a PVDF membrane in 10 mM 3-(cyclohexylamino)-1-propanesulfonic

acid buffer, pH 11, with 10% methanol. The membrane was rinsed in water (3 times, 5 min each), and the bands were identified by staining with Coomassie Brilliant Blue R-250. After washing with several changes of 50% methanol/10% acetic acid, a 63 kDa band was excised. The N-terminal amino acid sequence was determined by the University of Nebraska Medical Center Protein Structure Core Facility.

Circular Dichroism Measurements. A JASCO-J600 spectropolarimeter was used to record all CD spectra. The same sample was used for each Pr/Pfr combination, with photoconversion being performed in the sample compartment. Phytochrome concentrations from 0.17 to 0.19 mg/mL in 20 mM Tris, pH 7.8, containing 0.5 mM EDTA, and a 2 mm pathlength were used. Data were collected at 0.2 nm intervals from 200 to 250 nm. The apparent α-helix, β-sheet, β-turn, and random coil were estimated by the method of Chang et al. (1978) and Yang et al. (1986). This method was chosen because the solvent conditions limited the lower wavelength limit to 200 nm. The variable selection method (Manavalan & Johnson, 1987) is recommended only for data that go to at least 190 nm, with 184 nm being the preferred lower wavelength limit. Deforce et al. (1994) showed that secondary structure predictions made for phytochrome using the method of Yang et al. (1986) correlate well with results obtained using both the method of Manavalan and Johnson (1987) and convex constraint analysis as described by Perczel et al. (1992). Truncation of the spectra at 200 nm resulted in deviations from the magnitude of each component from that previously reported.

Fluorescence Quenching Measurements. Tryptophan fluorescence data were obtained by time-correlated single photon counting (O'Connor & Phillips, 1984) performed on an Edinburgh 299T fluorescence decay time spectrometer. The 292 nm excitation wavelength was produced by passing the light generated by a H_2 filled spark lamp through monochromators based on the EI-121 series. The emission wavelength, 350 nm, was selected in a similar fashion. A full-width at half-maximum of 1.0 ± 0.1 ns was maintained for all instrument profiles. Data analysis was accomplished using the Edinburgh FLA-900 fluorescence lifetime analysis package. Aliquots of a 5 M CsCl stock solution were added to phytochrome preparations of 0.1−0.4 A_{280}.

RESULTS

Phosphate Analysis of Untreated Phytochrome. Phosphate determination for oat phytochrome isolated as Pfr gave values ranging from 0.35 to 0.50 mol of phosphate/mol of monomer, with a sensitivity of 50 pmol of phosphate. The phosphate content of untreated phytochrome preparations was influenced to some extent by purification procedure. When initial purification steps (up to ASBE procedure which implies purification of phytochrome as Pfr) were performed with phytochrome as Pr, phosphate content of untreated preparations was approximately 40% lower than that for preparations purified as Pfr.

The exact nature of the phosphate linkage in untreated phytochrome is not known. In an attempt to identify the phosphoamino acid present in untreated phytochrome, both acid hydrolysis and monoclonal antibodies were used. Treatment of a 0.45 mol of phosphate/mol of phytochrome sample with 10 mM TCA at 90 °C to remove acyl phosphate and phosphoimidate resulted in only a 5−7% decrease in phosphate content, which was within the experimental error of the measurements. A BSA−phosphotyrosine conjugate was prepared (0.42 mol of phosphotyrosine residue/mol of BSA) to examine the presence of phosphotyrosine in the phytochrome samples. Using this positive standard, we detected by ECL analysis BSA−phosphotyrosine in a mixture containing 99% BSA and 1% BSA−phosphotyrosine conjugate. Furthermore, in a similar manner it was found that untreated phytochrome preparations contained no detectable phosphotyrosine, less than 0.005 mol/mol of monomer. Most likely, the phosphate is bound to the protein moiety by an ester bond with a serine residue.

Although no significant amount of acyl phosphate, phosphoimidate, or phosphotyrosine could be detected, it was found that the phosphate pool in untreated phytochrome was heterogeneous. Prostatic acid phosphatase in Tris-HCl buffer, pH 7.6 (under these conditions it has approximately 45% of the enzymatic activity found at pH optimal conditions, pH 5), removed less than half of the phosphate (initial phosphate content was 0.40 mol/mol of monomer, phosphate content of acid phosphatase-treated phytochrome was 0.25). Alkaline phosphatase was more effective for phytochrome dephosphorylation; phosphate content of phytochrome after incubation with alkaline phosphatase (30 min at room temperature as Pr and 30 min as Pfr) was below 0.03 mol/mol of phytochrome.

Preparation of Phosphorylated Phytochrome. Radioactive kinase assays showed that 0.90 and 0.65 mol of phosphate were incorporated into the Pr and Pfr forms after 1 h of phosphorylation at a PKA:phytochrome ratio of 1:75. Essentially the same values were obtained upon phosphate analyses of treated phytochromes obtained under the same reaction conditions using nonradioactive ATP (0.92 and 0.68 mol/mol of monomer incorporated for Pr and Pfr, respectively). Phytochrome pretreated with alkaline phosphatase (Pr and Pfr) showed essentially the same [^{32}P] incorporation after 1 h of incubation with PKA as did the Pr and Pfr forms of untreated phyA.

An increase in the enzyme:substrate ratio resulted in increased phosphorylation of both forms of untreated phytochrome and at an enzyme:substrate ratio of 1:20 Pr was phosphorylated up to 1.5 mol/mol of monomer, whereas 1.1 mol of phosphate incorporation was obtained for Pfr. Further increases of the enzyme:phytochrome ratio did not show a significant increase in phosphorylation. However, up to 1.8 mol of phosphate/mol of monomer could be incorporated into phytochrome when phytochrome phosphorylated as Pr for 45 min (enzyme:phytochrome ratio 1:20) was converted to Pfr by red light illumination and phosphorylated for an additional 45 min with fresh PKA.

Phytochrome samples phosphorylated as Pr with 0.92 mol of phosphate incorporated per mole of monomer, and as Pfr (0.68 mol/mol of monomer), were used in the present study. The phosphorylation conditions resulted in no detectable denaturation or degradation. All phosphorylated species were repurified from the reaction mixtures and analyzed by absorbance spectroscopy (photoreversibility conserved), SDS electrophoresis, and CD measurements. Furthermore, no dark reversion of Pfr after 1 h of phosphorylation (PKA:phytochrome ratio 1:75) was observed.

Our data on proteolytic digestion of untreated phytochrome as compared to those for phytochrome phosphorylated as Pr and as Pfr displayed some differences, but Pr phosphorylated

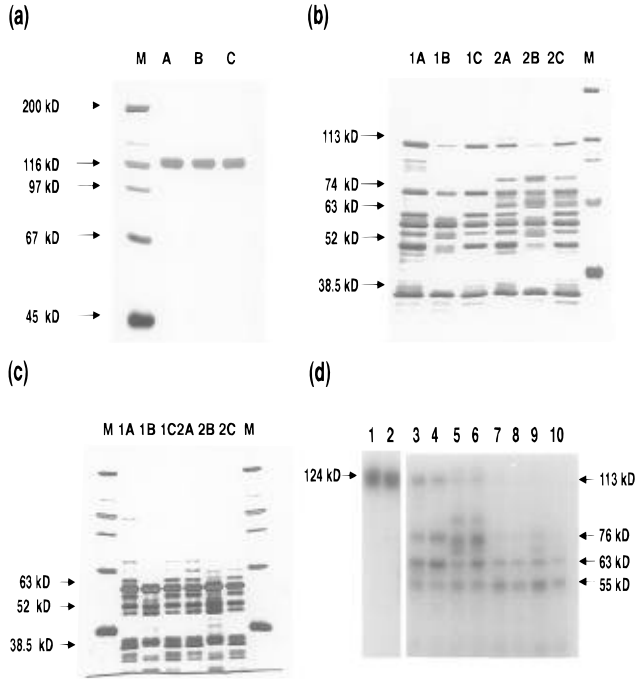

FIGURE 1: Comparative analysis of tryptic digest of phosphorylated and untreated phyA and confirmation of PKA phosphorylation sites. Phytochrome species were separated using 8% SDS−PAGE and then silver stained. (a) Undigested phytochrome, (b) 4 h digest, (c) 20 h digest. Lane labels are defined as follows: A, B, and C represent Pr phosphorylated, untreated, and Pfr phosphorylated phyA, respectively; 1 and 2 denote digested as Pr and digested as Pfr, respectively. (d) Autoradiogram of 4 h (lanes 3−6) and 20 h (lanes 7−10) tryptic digests. Undigested Pr and Pfr phosphorylated phytochrome, lanes 1 and 2; Pr phosphorylated phytochrome digested as Pr, lanes 3 and 7; Pfr phosphorylated phytochrome digested as Pr, lanes 4 and 8; Pr phosphorylated phytochrome digested as Pfr, lanes 5 and 9; Pfr phosphorylated phytochrome digested as Pfr, lanes 6 and 10.

and Pfr phosphorylated produced very similar proteolytic patterns. Autoradiography of the tryptic Pr digests (Figure 1d, lanes 3 and 4) for both phosphorylated species after 4 h of hydrolysis showed four distinct radiolabeled peptides at 113, 76, 63, and 55 kDa. Immunoblotting with N-terminal specific Oat-25 Mab revealed that these peptides did not contain the intact N-terminus (Figure 1b, lanes 1A and 1C; Figure 2b, lanes 1A and 1C, no positive band). The first three peptides were chromophore containing fragments [shown by Zn^{2+} fluorescence (data not shown) and immunoblotting with Oat-22 Mab (Figure 2a, lanes 1A and 1C)]. The 76-kDa fragment was likely a result of a cleavage at the Lys_{752}-Ala_{753} peptide bond. Sequence analysis of the 63-kDa fragment (Ser-Glu-Lys-Val-Ile and Val-Ile-Ala-Tyr-Leu) showed this fragment is a result of cleavage at the N-terminal trypsin-sensitive sites of Pr at Arg_{61}-Ser_{62} and Lys_{64}-Val_{65} and hydrolysis of the Arg_{623}-Leu_{624} peptide bond (determined from the molecular mass of this peptide). The 55-kDa fragment was recognized by Pea-25 Mab (Figure 2c, lanes 1A and 1C) and represents the C-terminal part of phytochrome. Phytochrome fragments are schematically shown in Figure 3.

Pfr digests of phosphorylated phytochromes produced more complicated autoradiographic patterns and showed several additional labeled fragments with the intact N-terminus (recognized by Oat-25 Mab, Figure 2b, lanes 2A and 2C) along with the previously mentioned peptides. Comparison of autoradiographic and immunoblot patterns

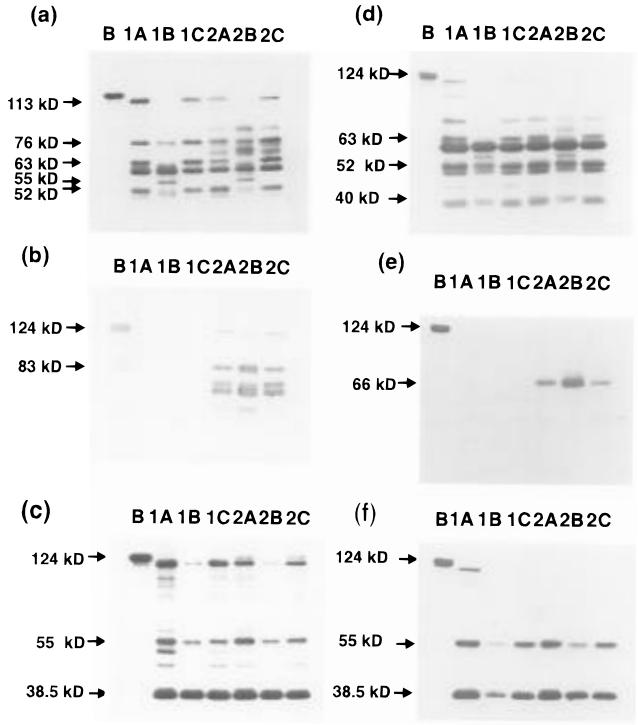

FIGURE 2: Immunoblot analysis of limited tryptic digest. Phytochrome species were digested with for 4 h (a, b, and c) and 20 h (d, e, and f). After separation by SDS−PAGE, peptides were transferred to nitrocellulose membrane and blotted with phyA Mab's (Oat-22 Mab, a and d; Oat-25 Mab, b and e; Pea-25 Mab, c and f) and then visualized by ECL. Lane labels are defined in Figure 1 with the exception of lane B, which is undigested untreated phyA used as a positive control for the Mab's.

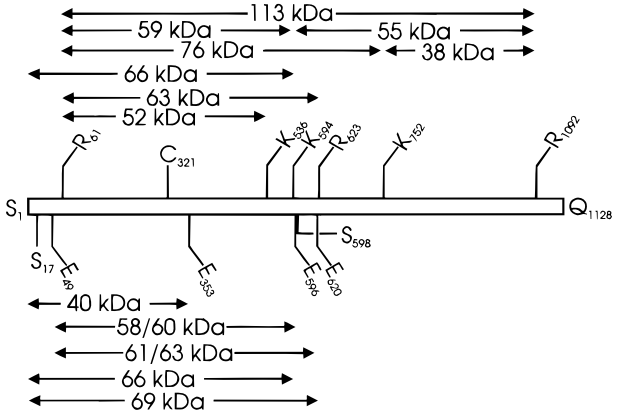

FIGURE 3: Schematic diagram of the limited proteolytic fragments from phyA. The bar in the middle represents the intact protein. The PKA phosphorylation sites, Ser_{17} and Ser_{598}, as well as the chromophore attachment site, Cys_{321}, are shown. The additional residues are sites of proteolytic attack and correspond to the peptides shown. Fragments above the central bar are from digestion with trypsin, and those below are from proteinase V8.

of the tryptic digest clearly showed that there are no other sites of PKA phosphorylation in the phytochrome molecule apart from N-terminus and the hinge region. A 59-kDa tryptic chromophore containing domain which was a main component of the 20 h digestion mixture (see Figure 1c, lanes 1A−2C) did not contain the [^{32}P]-label, but the 63-kDa fragment was labeled heavily. A 38.5-kDa C-terminal fragment (recognized by Pea-25 Mab, Figure 2c), which was formed easily at the initial stage of digestion and is from cleavage at Lys_{752}-Ala_{753}, did not contain the [^{32}P]-label, but the 55-kDa C-terminal fragment which includes the hinge

region was strongly labeled. So, labeling of the 113-, 76-, 63-, and 55-kDa fragments was a result of phosphorylation at the hinge region, and as an indication of phytochrome phosphorylation at the N-terminus, a labeled 66-kDa fragment with the intact N-terminus was observed (Figure 1d, lanes 5 and 6). The PKA phosporylation sites and protease fragmentation were in good agreement with previous reports (McMichael & Lagarias, 1990; Wong et al., 1986; Grimm et al., 1986, 1988).

It appears that Pr was also phosphorylated at the hinge region, resulting in similar proteolytic data for Pr and Pfr phosphorylated phytochromes. In order to more conclusively determine which of the two phytochrome forms was phosphorylated at the hinge region to a greater extent, equal amounts of Pr and Pfr phosphorylated phytochrome, digested as Pr by trypsin for 4 h, were applied to SDS−PAGE and then transferred to a nitrocellulose membrane. Four bands which include the [^{32}P]-label as a result of phosphorylation only at the hinge region (113-, 74-, 63-, and 55-kDa) were cut from the membrane and measured for radioactivity. It was found that Pfr has only a slightly higher preference for phosphorylation at the hinge region. The ratio Pfr-phosphate/Pr-phosphate was around 1.3. This is not unexpected if we take into account that the hinge region is exposed in both the Pfr and the Pr phytochrome forms.

Pr showed a much stronger preference for phosphorylation at the N-terminus as compared to Pfr. This was confirmed by radioactivity measurements of a 40-kDa fragment with the intact N-terminus derived from Pfr digests of Pr and Pfr phosphorylated phytochromes by proteinase V8. In spite of the fact that Pr phosphorylated phytochrome produced a smaller quantity of the peptide as compared with Pfr phosphorylated (and untreated phytochrome, Figure 4b, lanes 2A and 2C), the radioactivity of this peptide band for Pr phosphorylated phytochrome was 2.2 times higher than one measured for Pfr phosphorylated phytochrome. It should be pointed out that autoradiographic data on tryptic digest for phosphorylated phytochrome, originally isolated from etiolated tissue as Pr, were similar to those described for phytochrome isolated as Pfr.

CD Analysis. The secondary structures of the photoreversible forms of phytochrome are shown in Figure 5. The spectral data for untreated phytochrome and phytochrome phosphorylated as Pr are shown in Figure 5, panels a and c, respectively. In general, the spectra of corresponding light absorbing forms have the same shape and within the limits of the noise are superimposable upon each other. A similar trend is observed for both phytochrome phosphorylated as Pfr and dephosphorylated phytochrome. In general, the state of phosphorylation has no CD detectable influence on the secondary structure, as is illustrated in Figure 5. The red light induced increase in α-helix at the expense of random coil and β-turn was reproducible regardless of the phosphorylation state of the phytochrome. A net gain of approximately 3% helical structure, corresponding to a 10% change in the CD signal, was observed upon photoconversion of all Pr species to Pfr. This elevation in the extent of helical structure was however reversed by far-red light initiated back transformation to Pr.

As was the case for the CD measurements, results from subsequent analysis by fluorescence quenching and limited proteolysis of dephosphorylated phytochrome were indistinguishable from those for untreated phytochrome. In light

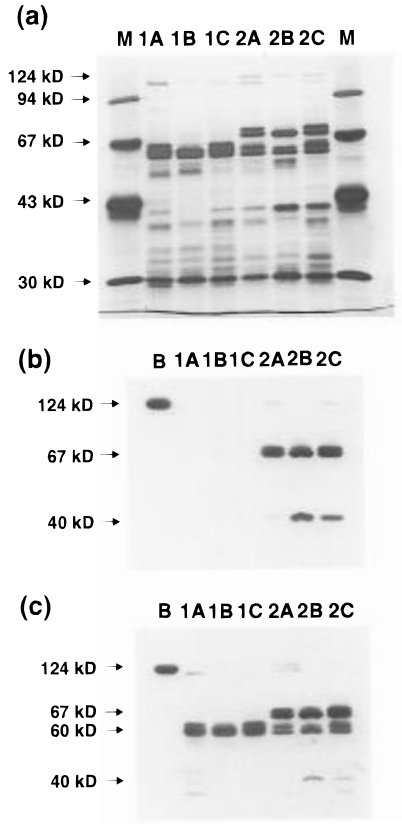

FIGURE 4: 24 h proteinase V8 digest of phosphorylated and untreated phyA. After digestion, samples were separated by 10% SDS−PAGE. (a) Silver stained gel; (b) and (c) are the digest blotted with Oat-25 Mab and Oat-22 Mab, respectively. Lane labels are defined in Figure 1 with the exception of lanes B and M. The former is undigested Pr phosphorylated phyA, a positive control, and the latter is the molecular weight markers.

of this and the previously discussed similarity between the level of [^{32}P] incorporation of dephosphorylated phyA and untreated phyA, only untreated and PKA phosphorylated samples will be discussed further.

Fluorescence Quenching Measurements. The microenvironments around the 10 Trp's contained in phytochrome are sensitive to the red light induced photoisomerization of the tetrapyrollic chromophore. In previous studies, it was demonstrated that dynamic fluorescence quenchers such as Tl^+, Cs^+, I^-, and acrylamide were able to reveal conformational changes, and established that the surface topography and packing density of Pr differ significantly from that of Pfr (Singh & Song, 1990; Wells et al., 1994). In the present study, because of its large ionic radius (1.67 Å), we decided to use Cs^+ to probe for conformational changes associated with the addition of phosphate groups at Ser_{17} and Ser_{598}.

The analysis of all fluorescence decays was performed by reconvolution fit using the Marquardt search algorithm. Satisfactory fits were obtained using a two exponential model, as determined by randomly distributed residuals and χ^2's between 0.8 and 1.2. Fitting of the fluorescence decays yielded lifetimes of 1.22 and 4.79 ns for Pr and 1.23 and 4.95 ns for Pfr.

Figure 6 shows the results of stepwise addition of 5 M CsCl stock solution on the decay time of the Trp fluorescence. Although the Stern−Volmer constants (Table 1) were lower than those obtained by Singh and Song (1990), due to different sample conditions and decay measurements, the general trend of the short component being more accessible

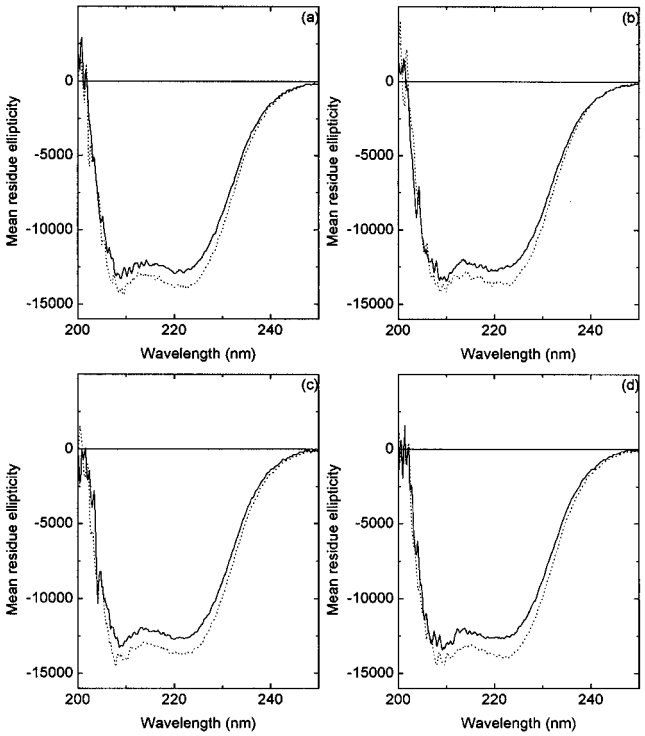

FIGURE 5: Far-UV CD spectra of (a) untreated phytochrome A, (b) phytochrome dephosphorylated with alkaline phosphatase, (c) phyA phosphorylated as Pr, and (d) phyA phosphorylated as Pfr. In (a−d) both the Pr (—) and Pfr (···) photoisomers are shown. For Pr the fractional contributions of α-helix = 0.40, β-sheet = 0.00, β-turn = 0.21, and random structure = 0.39 in (a) through (d). For Pfr α-helix = 0.43, β-sheet = 0.00, β-turn = 0.19, and random structure = 0.38 (a)−(d).

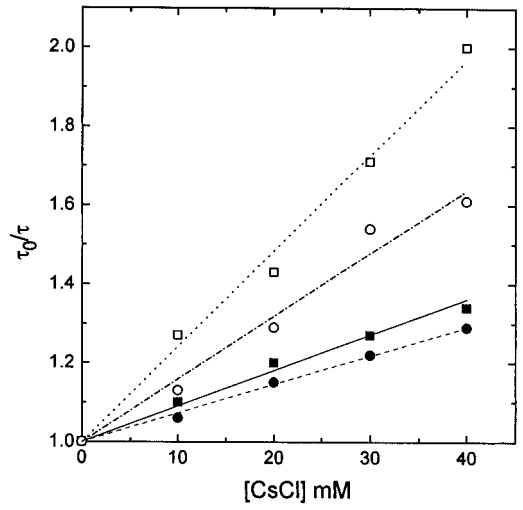

FIGURE 6: Stern−Volmer plots for Cs^+ quenching of the short tryptophan lifetime component of untreated phytochrome and phytochrome phosphorylated as Pr. Untreated Pr (■), Pfr (●); Pr phosphorylated Pr (□), Pfr (○). A sample temperature of 277 K was maintained throughout.

in Pr and the long component being more accessible in Pfr was confirmed for the untreated species in 20 mM Tris. Phosphorylation either as Pr or Pfr resulted in an increase in the short component Stern−Volmer constants for both photoisomers (Table 1), yet the trends were the same as for untreated phytochrome. Phosphorylation of either Pr or Pfr did not seem to affect the long component K_{sv}'s drastically, but Pr does seem to be preferentially quenched compared to Pfr (Table 1). In general, tryptophans in Pr phosphorylated

Table 1: The Stern−Volmer Quenching (K_{sv}, M^{-1}) and Rate (k_q, M^{-1} s^{-1} x 10^{-9}) Constants for Untreated Phytochrome A, PhyA Phosphorylated as Pr, and PhyA Phosphorylated as Pfr Trp Fluorescence Quenching (Cs^+ Ions as Quencher)

	τ_1		τ_2	
	K_{sv}	k_q	K_{sv}	k_q
untreated Pr[a]	9.0	7.4	5.6	1.2
untreated Pfr[a]	7.3	5.9	6.6	1.3
phosphorylated as Pr, Pr[a]	24.2	18.6	8.3	1.8
phosphorylated as Pr, Pfr[a]	15.9	12.9	7.9	1.7
phosphorylated as Pfr, Pr[a]	19.3	16.4	6.8	1.6
phosphorylated as Pfr, Pfr[a]	12.1	10.3	6.4	1.4

[a] The light absorbing form of phytochrome used during the decay measurements.

phytochrome were more accessible to Cs^+ than those in Pfr phosphorylated phytochrome.

Limited Proteolysis of Phytochrome Preparations. We used limited proteolysis under mild conditions with trypsin at an enzyme:substrate ratio of 1:2000 and with glutamic acid specific proteinase V8 as probes for changes in surface accessibility introduced by phosphorylation. As the number, size, and relative quantity of proteolytic fragments are strongly dependent on the digestion conditions, we performed a comparative analysis of different phytochrome species in parallel experiments under the same conditions. Most of the protease-sensitive sites of native phytochrome were described previously (Lagarias & Mercurio, 1985; Grimm et al., 1986, 1988), but different phytochrome species displayed to some extent different behavior as for their preferential cleavage sites.

Analysis of Tryptic Digest of PKA Phosphorylated Species. Under mild digestion conditions, several easily accessible cleavage sites were found for untreated Pr phytochrome. They include the Lys_{64}-Val_{65}, Arg_{61}-Ser_{62}, and Lys_{752}-Ala_{753} peptide bonds. Another pathway of tryptic digestion was cleavage at the hinge region rather than at Lys_{752}-Ala_{753}, ultimately forming a 55-kDa C-terminal fragment (Figure 3). As a result of splitting at the above locations, 76-kDa, 59-kDa, 38.5-kDa, and 55-kDa peptides were observed after 10 min, 1 h (data not shown), and 4 h of digestion (Figure 1b, lane 1B). Pfr on the other hand lost the N-terminal region less readily, and an 83-kDa fragment as well as a 66-kDa peptide, both with the intact N-terminus, were present in the 4 h digest (Figure 1b, lane 2B). Differences of tryptic patterns for phosphorylated phytochrome species and untreated phytochrome were observed at the initial stages of tryptic digestion, whereas no significant differences between Pfr and Pr phosphorylated phytochrome were found. This was expected, though, in light of the fact that both Pr and Pfr are phosphorylated in the hinge region.

The main cleavage sites of the Pr and Pfr forms were not affected significantly by phosphorylation, but the total rate of hydrolysis at some sites was lower for the phosphorylated species. For example, a larger quantity of undigested 113-kDa fragment was detected from the phosphorylated species after 4 h of incubation (Figure 1b) as compared with that for the untreated protein. The 4 h digest clearly showed formation of an increased amount of a 52-kDa chromophore fragment recognized by the Oat-22 Mab (Figure 2a, compare lanes 1A, 1C and 2A, 2C with lanes 1B and 2B). This 52-kDa fragment was a result of a cleavage of the N-terminus and the Lys_{536}-Asn_{537} peptide bond as noted by Grimm et

al. (1986). Also as a result of the increased sensitivity of this peptide bond to tryptic digestion, the phosphorylated species after 10−20 min of hydrolysis produced a short-lived 61.5-kDa C-terminal fragment, recognized by Pea-25 Mab (data not shown). Untreated phytochrome, in turn, produced a 55-kDa chromophore fragment (cleavage of the Lys_{564}-Ser_{565} peptide bond), as described previously by Grimm et al. (1986) (see Figure 2a, lanes 1B and 2B), which in turn was not detected for the phosphorylated species. Furthermore, phosphorylation at the N-terminus (Ser_{17}) did not interfere with the high susceptibility of the N-terminal region for tryptic cleavage. Pr phosphorylated phytochrome lost its N-terminus as readily as untreated phytochrome did. Most likely, Ser_{17} and the tryptic-sensitive surface exposed sites are spatially remote from each other.

Several sites C-terminal to the hinge region also had altered accessibility to trypsin as a result of phosphorylation. Immunoblot analysis of the 4 h digest with Pea-25 Mab revealed the formation of 52- and 47-kDa fragments from the phosphorylated phytochrome species (Figure 2c, lanes 1A, 1C, 2A, and 2C). The 52-kDa C-terminal fragment was a result of cleavage at Agr_{623}-Leu_{624} (Grimm et al., 1986). Exposure of this peptide bond also caused formation of a 63-kDa chromophore domain fragment as mentioned earlier. Differences between the proteolytic patterns of phosphorylated phytochromes and untreated phytochrome were still present after 20 h of digestion (fragment with molecular mass 63 kDa, Figure 1c).

Analysis of Proteinase V8 Digests. Likewise, untreated phytochrome (in Pr and in Pfr forms) was digested by proteinase V8 more readily than phosphorylated phytochrome preparations. 24 and 48 h digestion clearly displayed the differences between the Pr and Pfr forms of native phytochrome as reported earlier by Grimm et al. (1988). They found that Pr to Pfr phototransformation exposed to the surface a site located remarkably close to the chromophore (Glu_{353}-Gln_{354} peptide bond). We confirmed that formation of the 40-kDa fragment was a result of conformational changes at the site around Glu_{353}-Gln_{354} by immunoblotting with Oat-25 Mab (Figure 3a, compare lanes 2B and 1B). This 40-kDa N-terminal Pfr specific domain was formed in a significant amount after 24 h of digestion with proteinase V8. Pr digest did not produce a equivalent fragment without the N-terminal 6-kDa portion.

It is interesting to note that formation of the Pfr specific 40-kDa chromophore fragment was inhibited for phosphorylated phytochromes, especially for phytochrome phosphorylated as Pr. The slight decrease in formation of the 40-kDa fragment for Pfr phosphorylated phytochrome was probably a result of the presence of at least 12% Pr in all Pfr samples.

Proteinase V8, which cleaves the peptide bond at the C-terminus of negatively charged amino acids (Glu, Asp), easily splits the Glu_{596}-Ala_{597} peptide bond in untreated phytochrome (in Pr and Pfr forms). Phosphorylation at the hinge region makes this peptide bond more resistant to digestion, and a number of chromophore fragments with increased molecular mass (by approximately 3 kDa) were obtained for phosphorylated species as compared with untreated phytochrome. The phosphorylation site is located at this easily cleaved site, and most likely attachment of the phosphate group to Ser_{598} results in interference of enzyme interaction with peptide bonds in this region. Digests of phosphorylated (as Pr or Pfr) phytochromes resulted in formation of additional 69- and 63-kDa peptides corresponding to Pfr and Pr digest, respectively (Figure 4a, 3b, 3c). Obviously, formation of these peptides was caused by protection of Glu_{596}-Ala_{597} by the phosphate group at Ser_{598} or by phosphorylation-induced local conformation changes at the hinge region residues. The C-terminal domain of each phytochrome species was more readily hydrolyzed than the N-terminal domain, and after 24 h of digestion no large peptides were identified by Pea-25 Mab.

DISCUSSION

Initially, we thought that phosphorylation of Ser_{17} would perturb the conformation of the N-terminal segment of phytochrome which forms an amphiphilic α-helical fold upon Pr→Pfr phototransformation (Parker & Song, 1990, 1992; Parker et al., 1992; Deforce et al., 1994). Functional studies of this region imply that alteration of the α-helix could have significant effects on phytochrome activity (Cherry et al., 1992; Stockhaus et al., 1992; Boylan et al., 1994). In the present study, it has been demonstrated that phosphorylation of Ser_{17} and/or Ser_{598} has no detectable impact on secondary structure as determined by circular dichroism. The 10% CD signal increase at 222 nm and 3% elevation in helix upon photoconversion to Pfr were conserved for all phyA tested, regardless of the state of phosphorylation. The absence of a phosphorylation-induced CD variation leaves tertiary rearrangement as the most probable form of conformational change, unlike the myelin basic protein in which almost the entire β-structure of the protein is not only induced but maintained by phosphorylation (Ramwani et al., 1989).

The 10 conserved tryptophans contained within phyA's primary structure have been exploited as probes for topographic rearrangement resulting from Pr to Pfr phototransformation (Sarkar & Song, 1982; Singh et al., 1988, 1989; Singh & Song, 1990; Mizutani et al., 1993; Toyama et al., 1993; Wells et al., 1994). A measurable photoisomer-specific difference in the exposure of these residues to dynamic fluorescence quenchers (Singh et al., 1988; Singh & Song, 1990; Wells et al., 1994), attributed to microenvironmental changes surrounding them (Wells et al., 1994), has been clearly shown. Here we probed similar conformational changes modulated by PKA phosphorylation events. The quencher chosen was Cs^+ because its ionic radius is large and it shows differential quenching behavior with respect to the short and long lifetime components (Singh & Song, 1990; Wells et al., 1994).

Phosphorylation-induced changes in the short component of the Trp fluorescence decay were confined to increases in quencher accessibility with retention of Pr having the more accessible indolic residues. There was, however, a reversal of the quenching behavior for the long component of the tryptophan fluorescence. However, because the differences in Stern−Volmer constants are small it is difficult to attribute them to significant changes in the surface topography of the protein. The changes observed did occur for both phytochrome phosphorylated as Pr and phosphorylated as Pfr and, therefore, must be a result of phosphorylation at Ser_{598}. The behavior of both short and long component quenching may also stem from the increased negative charge as a result of phosphorylation; this would raise the local concentration of Cs^+ in the areas around Ser_{17} and Ser_{598} and affect the vicinal

Trp's fluorescence, due to the electrostatic interaction between the ion and the charged residues. The likelihood that 2 phosphate groups could, via electrostatic interactions, affect all 10 Trp's spread throughout the protein is very unlikely though.

Differences in proteolytic patterns between phosphorylated phytochrome species and untreated phyA were observed at the initial stages of tryptic digestion, whereas no significant differences between Pr and Pfr phosphorylated phytochrome were found. The latter is to be expected though, in light of the fact that both photoisomers were phosphorylated in the hinge region. Wong et al. (1986) also mentioned that tryptic peptide patterns were not dependent upon the form of phytochrome used for phosphorylation. Furthermore, trypsin and V8 digestion patterns for untreated phyA and dephosphorylated phyA were indistinguishable.

Phosphorylation at the hinge region (Ser_{598}) resulted in more noticeable changes in the phytochrome proteolytic pattern (with trypsin and proteinase V8) than phosphorylation at the N-terminus. Phosphorylation at Ser_{598} exposes some sites to trypsinolysis and inhibits both trypsin and V8 enzymatic attack at other sites. Trypsin attack at Lys_{536} and Arg_{623} was elevated in phosphorylated phytochrome, but the peptide bond at Lys_{564} was blocked by phosphorylation. It is also possible that cleavage at Lys_{536} became so efficient that the 55-kDa fragment which resulted from cleavage at Lys_{564} was rapidly degraded and therefore no longer observed for phosphorylated phytochrome. Glu_{596} was more resistant to glutamic proteinase V8 digestion after coupling of the phosphate group to its neighbor, Ser_{598}. The combined trypsin and proteinase V8 data suggest that phosphorylation of Ser_{598} modulates the protease accessibility from at least Lys_{536} to Arg_{623} and possibly beyond. The inhibition of V8 cleavage at Glu_{596} was probably also due to electrostatic or steric blocking of the peptide bond by the phosphate group at Ser_{598} rather than conformational change. Changes in typsin digestion may have also resulted from similar means. However, conformational change seems the most plausible because electrostatic interactions are local phenomena.

Phosphorylation of Ser_{17} affects proteinase V8 cleavage at a site remote from it in the primary structure, suggesting that the N-terminus is positioned near Glu_{354} or that it is translocated there upon phosphorylation as in glycogen phosphorylase. Phosphorylation of glycogen phosphorylase results in translocation of Ser_{14}, the site of phosphorylation, more than 36 Å to where it then interacts with the C-terminal domain at residues 838−842, resulting in an order−disorder transition of this region (Johnson & Barford, 1993). Another alternative is that phosphorylation at Ser_{17} disrupts some other region and the resulting strain is transmitted to this region. In myosin II the phosphorylation-induced changes are quite subtle. The increased negative charge upon phosphorylation causes the short tailpieces of the filamentous protein to repel each other. The resulting strain is transmitted through a helix and changes the endopeptidase Arg-C accessibility of the N-terminal globular heads (Redowicz et al., 1994).

Although cAMP-dependent protein kinase can phosphorylate phytochrome at Ser_{17} (Pr) and Ser_{598} (Pfr 1.3 times greater than Pr), the presence of PKA has not been conclusively shown in plants. However, there is evidence suggesting that "PKA-like" proteins are present. Several PKA homologs have been cloned from plants, but their protein function has yet to be elucidated (Assmann, 1995). A partially purified kinase from petunia has been found to phosphorylate the kemptide (LPRASLG), a synthetic substrate for PKA (Polya et al., 1991). Animal PKA has been shown to mimic in vivo phosphorylation of the α-tonoplast intrinsic protein channel, resulting in a doubling of the conductance of the seed-specific vacuolar water channel (Maurel et al., 1994). Furthermore, adenylate cyclase activity in etiolated oat seedling crude extracts has been shown to be red/far-red light regulated (Hahn et al., 1991). The red light induced increase in adenylate cyclase activity implies not only the presence of PKA but also a connection between it and phytochrome-mediated signal transduction. Another possibility is that PKA is mimicking a calcium-dependent protein kinase (Assmann, 1995). Some calcium-dependent protein kinases phosphorylate peptides that are also phosphorylated by PKA. Ca^{2+} has been shown to simulate phytochrome-regulated gene expression (Lam et al., 1989; Tretyn et al., 1991; Neuhaus et al., 1993; Bowler et al., 1994). It remains to be seen if PKA and the accessibility differences induced by its catalysis of Ser_{17} and Ser_{598} phosphorylation are involved in phyA-mediated signaling.

CONCLUDING REMARKS

In this study, we used the PKA-catalyzed phosphorylation to probe for possible conformational changes in phytochrome as modulated by the post-translational modification. From the present results, we conclude that phosphorylation may be Pr- and Pfr-dependent and that phosphorylation most likely induces subtle conformational changes in Pr and Pfr. It appears that PKA phosphorylation of phytochrome at both Ser_{17} and Ser_{598} is "nonsilent".

REFERENCES

Akhrem, A. A., & Drozhdenyuk, A. P. (1989) *Anal. Biochem. 179*, 86−89.

Assmann, S. M. (1995) *Plant Physiol. 108*, 885−889.

Benovic, J. L., DeBlasi, A., Stone, W. C., Caron, M. G., & Lefkowitz, R. J. (1989) *Science 246*, 235−246.

Benovic, J. L., Onorato, J. J., Arriza, J. L., Stone, W. C., Loshe, M., Jenkins, N. A., Gilbert, D. J., Copeland, N. G., Caron, M. G., & Lefkowitz, R. J. (1991) *J. Biol. Chem. 266*, 14939−14946.

Biermann, B. J., Pao, L. I., & Feldman, L. J. (1994) *Plant Physiol. 105*, 243−251.

Blum, H., Beier, H., & Goss, H. J. (1987) *Electrophoresis 8*, 93−99.

Bowler, C., Yamagata, H., Neuhaus, G., & Chua, N.-H. (1994) *Genes Dev. 8*, 2188−2202.

Boylan, M., Douglas, N., & Quail, P. H. (1994) *Plant Cell 6*, 449−460.

Bradford, M. (1976) *Anal. Biochem. 72*, 248−254.

Buss, J. E., & Stull, J. T. (1983) *Methods Enzymol. 99*, 7−16.

Cherry, J. R., Hondred, D., Walker, J. M., & Vierstra, R. D. (1992) *Proc. Natl. Acad. Sci. U.S.A. 89*, 5039−5043.

Deforce, L., Tokutomi, S., & Song, P.-S. (1994) *Biochemistry 33*, 4918−4922.

Fletcher, W. M., Van Patten, S. M., Cheng, H.-C., & Walsh, D. A. (1986) *J. Biol. Chem. 261*, 989−992.

Furuya, M. (1993) *Annu. Rev. Plant Physiol. Plant Mol. Biol. 44*, 617−645.

Grimm, R., Lottspeich, F., Schneider, H. A. W., & Rüdiger, W. (1986) *Z. Naturforsch. 41c*, 221−223.

Grimm, R., Eckerskorn, C., Lottspeich, F., Zenger, C., & Rüdiger, W. (1988) *Planta 174*, 396−401.

Grimm, R., Gast, D., & Rüdiger, W. (1989) *Planta 178*, 199−206.

Hahn, T. R., & Song, P.-S. (1991) *Photochem. Photobiol. 53*, 12S.

Hershey, H. P., Barker, R. F., Idler, K. B., Lissemore, J. L., & Quail, P. H. (1985) *Nucleic Acids Res. 13*, 8543−8559.

Hunt, R. E., & Pratt, L. H. (1980) *Biochemistry 19*, 390−394.

Johnson, L. N., & Barford, D. (1993) *Annu. Rev. Biophys. Biomol. Struct. 22*, 199−232.
Kim, I. S., Bai, U., & Song, P.-S. (1989) *Photochem. Photobiol. 49*, 319−323.
Laemmli, U. K. (1970) *Nature 227*, 680−685.
Lagarias, J. C., & Mercurio, F. M. (1985) *J. Biol. Chem. 260*, 2415−2423.
Lagarias, J. C., Kelly, J. M., Cyr, K. L., & Smith, W. O., Jr. (1987) *Photochem. Photobiol. 46*, 5−13.
Lam, E., Benedyk, M., & Chua, N.-H. (1989) *Mol. Cell. Biol. 9*, 4819−4823.
Lapko, V. N. (1989) *Izvest. Acad. Nauk. BSSR, Ser. Biol. 2*, 104−107.
Lapko, V. N., & Song, P.-S. (1995) *Photochem. Photobiol. 62*, 194−198.
Manavalan, P., & Johnson, W. C., Jr. (1987) *Anal. Biochem. 167*, 76−85.
Maurel, C., Kado, R. T., Guern, J., & Chrispeels, M. J. (1994) in *Proceedings Vth International Symposium of Plant Molecular Biology*, International Society for Plant Molecular Biology, Amsterdam, Abstract 1009.
McMichael, R. W., Jr., & Lagarias, J. C. (1990) *Biochemistry 29*, 3872−3878.
Mitchell, D. C., Kibelbek, J., & Litman, B. J. (1992) *Biochemistry 31*, 8107−8111.
Mizutani, Y., Tokutomi, S., Kaminaka, S., & Kitagawa, T. (1993) *Biochemistry 32*, 6916−6922.
Neuhaus, G., Bowler, C., Kern, R., & Chua, N.-H. (1993) *Cell 73*, 937−952.
O'Connor, D. V., & Phillips, D. (1984) *Time-Correlated Single Photon Counting*, Academic Press, Orlando, FL.
Park, H. J., & Song, P.-S. (1990) *Photochem. Photobiol. 51*, 8−9S.
Parker, W., & Song. P.-S. (1990) *J. Biol. Chem. 265*, 17568−17575.
Parker, W., & Song. P.-S. (1992) *Biophys. J. 61*, 1435−1439.
Parker, W., Partis, M., & Song. P.-S. (1992) *Biochemistry 31*, 9413−9419.
Perczel, A., Park, K., & Fasman, G. D. (1992) *Anal. Biochem. 203*, 83−93.
Polya, G. M., Chung, R., & Menting, J. (1991) *Plant Sci. 79*, 37−45.
Pratt, L. H. (1982) *Annu. Rev. Plant Physiol. 33*, 557−582.
Pratt, L. H., Cordonnier, M.-M., & Lagarias, J. C. (1988) *Arch. Biochem. Biophys. 267*, 723−735.
Quail, P. H. (1991) *Annu. Rev. Genet. 25*, 389−409.
Quail, P. H., Briggs, W. R., & Pratt, L. H. (1978) in *Carnegie Institution Annual Report, Dept. of Plant Biology*, pp 342−344, Carnegie Institute of Washington, Stanford, CA.
Quail, P. H., Boylan, M. T., Parks, B. M., Short, T. W., Xu, Y., & Wagner, D. (1995) *Science 268*, 675−680.
Ramwani, J. J., Epand, R. M., & Morcarello, M. (1989) *Biochemistry 28*, 6538−6543.
Redowicz, M. J., Martin, B., Zolkiewski, M., Ginsburg, A., & Korn, E. D. (1994) *J. Biol. Chem. 269*, 13558−13563.
Romero, L. C., Biswal, B., & Song, P.-S. (1991a) *FEBS Lett. 282*, 347−350.
Romero, L. C., Sommer, D., Gotor, C., & Song, P.-S. (1991b) *FEBS Lett. 282*, 341−346.
Roskoski, R., Jr. (1983) *Methods Enzymol. 99*, 3−7.
Sarkar, H. K., & Song, P.-S. (1982) *Biochemistry 21*, 1967−1972.
Singh, B. R., & Song, P.-S. (1990) *Photochem. Photobiol. 52*, 249−254.
Singh, B. R., Chai, Y. G., Song, P.-S., Lee, J., & Robinson, G. W. (1988) *Biochim. Biophys. Acta 936*, 395−405.
Singh, B. R., Choi, J., Kwon, T., & Song, P.-S. (1989) *J. Biochem. Biophys. Methods 18*, 135−148.
Sommer, D. (1993) Ph.D. Dissertation, University of Nebraska−Lincoln.
Sommer, D., & Song, P.-S. (1994) *Protein Purification & Expression 5*, 402−408.
Sommer, D., Romero, L., & Song, P.-S. (1991) *Photochem. Photobiol. 53*, 12S.
Stockhaus, J., Nagatani, A., Halfter, U., Kay, S., Furuya, M., & Chua, N.-H. (1992) *Genes Dev. 6*, 2364−2372.
Toyama, A., Nakazawa, M., Manabe, K., Takeuchi, H., & Harada, I. (1993) *Photochem. Photobiol. 52*, 391−395.
Tretyn, A., Kendrick, R. E., & Wagner, G. (1991) *Photochem. Photobiol. 54*, 1135−1155.
Van Etten, R. L. (1978) *Clin. Chem. 24*, 1255−1259.
Wells, T. A., Nakazawa, M., Manabe, K., & Song, P.-S. (1994) *Biochemistry 33*, 708−712.
Wilden, U., & Kuhn, H. (1982) *Biochemistry 21*, 3014−3022.
Wong, Y.-S., Cheng, H.-C., Walsh, D. A., & Lagarias, J. C. (1986) *J. Biol. Chem. 261*, 12089−12097.
Yang, J. T., Wu, C.-S. C., & Martinez, H. M. (1986) *Methods Enzymol. 130*, 208−269.

BI9529364